Caloric effects induced by magnetic and mechanical fields in a $Ni_{50}Mn_{25-x}Ga_{25}Co_x$ magnetic shape memory alloy

P. O. Castillo-Villa, D. E. Soto-Parra, J. A. Matutes-Aquino, and R. A. Ochoa-Gamboa
Centro de Investigación en Materiales Avanzados, S.C. Miguel de Cervantes 120, Complejo Industrial Chihuahua, 31109 Chihuahua, México

Antoni Planes, Lluís Mañosa, and David González-Alonso
Departament d'Estructura i Constituents de la Matèria, Facultat de Física, Universitat de Barcelona, Diagonal 647, E-08028 Barcelona, Catalonia, Spain

Marcelo Stipcich
IFIMAT, Universidad Nacional del Centro de la Provincia de Buenos Aires, Pinto 399, 7000 Tandil and Consejo Nacional de Investigaciones Científicas y Técnicas, A. Rivadavia 1917, Buenos Aires, Argentina

Ricardo Romero
IFIMAT, Universidad Nacional del Centro de la Provincia de Buenos Aires and CICPBA, Pinto 399, 7000 Tandil, Argentina

D. Ríos-Jara and H. Flores-Zúñiga
Instituto Potosino de Investigación Científica y Tecnológica, Camino a la Presa, 2055 Col. Lomas 4a CP, 78216 San Luis Potosí, México
(Received 22 December 2010; revised manuscript received 19 February 2011; published 16 May 2011)

We have studied the elastocaloric effect in a Co-doped Ni-Mn-Ga magnetic Heusler shape memory alloy in the vicinity of its martensitic transition. Measurements of the length change as a function of temperature have been carried out across the transition under applied compression stresses and magnetic fields. The isothermal stress-induced entropy changes have been computed from the experimental data. Results evidence a significant elastocaloric effect associated with the large entropy change of the structural phase transition. The alloy also exhibits a magnetocaloric effect at low applied magnetic fields. It is shown that application of a magnetic field below 1 T increases the estimated elastocaloric relative cooling power by about 20%. A comparison of elasto- and magnetocaloric properties indicates that a similar relative cooling power is reached under application of 10 MPa or 0.8 T.

DOI: 10.1103/PhysRevB.83.174109 PACS number(s): 81.30.Kf, 64.60.My, 75.30.Sg

I. INTRODUCTION

Caloric effects originating from the thermal response to changes of external fields such as mechanic, electric, or magnetic fields are inherent to every material.[1] They are typically quantified either by the adiabatic temperature change or by the isothermal entropy change that occurs upon application or removal of an external field.[2] Materials displaying large caloric effects are recently receiving a great deal of attention since they are promising candidates for environmental-friendly refrigeration techniques.[3–6] At present, the most studied caloric effect is the magnetocaloric effect. After the discovery in the mid-1990s of materials displaying giant magnetocaloric effect in the vicinity of room temperature[7] a large amount of research has been carried out on this topic.[8–11] In addition, in recent years other caloric effects such as the electrocaloric,[12] elastocaloric,[13,14] and barocaloric[15] effects have received increasing attention. A key feature common to most materials showing a giant caloric effect is the occurrence of a first-order phase transition. The expected large (discontinuous) change of the order parameter at the transition involves a large entropy content (associated with the latent heat) which is at the origin of the giant caloric effect. In addition, strong coupling between different degrees of freedom such as structural, magnetic, electric, etc. enables the transition to be driven by the different fields conjugated to the corresponding extensive property, and several caloric effects are expected to occur in an interdependent way.

In the present paper we focus on the influence of a magnetic field on the mechanic-caloric effects in Heusler shape memory alloys. These systems are ferromagnetic materials that undergo a martensitic transition responsible for shape memory properties.[16] They display strong coupling between structural and magnetic properties that enables large deformations to be induced by application of moderate magnetic fields.[17–20] Therefore, in the vicinity of the structural transition, large changes of entropy are expected to occur under application of mechanical and magnetic fields. Typically, the mechanical field corresponds to an applied hydrostatic pressure or to a uniaxial stress. In the former case, the caloric effect is called barocaloric, while in the second case it is denoted as the elastocaloric effect. An interesting feature regards the fact that in these magnetic shape memory materials the interplay between structure and magnetism occurs at two well-separated length scales.[16,21] At the scale of the martensitic variants it is controlled by the increase of magnetocrystalline anisotropy taking place at the transition from the high to the low symmetry phases. At a more microscopic length scale, it is controlled by the corresponding change of the effective magnetic exchange. The first contribution is essentially responsible for the magnetic shape memory effect, while the second makes magnetic

superelasticity feasible (possibility of magnetically inducing the structural transition[19,20]). Both contributions are expected to give rise to the caloric properties of this kind of materials.

The present work is aimed at studying the elastocaloric properties of a Ni-Mn-Ga-Co Heusler alloy and their relation to its magnetocaloric properties from magnetothermomechanical and calorimetric experiments. Special emphasis has been devoted to the analysis of the influence of the magnetostructural coupling in these caloric properties. The studied alloy has a composition close to the line $Ni_{50}Mn_{25-x}Ga_{25}Co_x$. In this family the effect of Co substitution is to increase the temperature of the martensitic transition which becomes closer to the Curie point. Interestingly, this substitution keeps the entropy difference between the parent and martensitic phases almost unaffected.[22]

The paper is organized as follows. In Sec. II we briefly develop the thermodynamics equations describing caloric effects in systems with magnetostructural coupling. In Sec. III the experimental setup, sample characteristics, and methods are described. The obtained experimental results are presented and briefly discussed in Sec. IV. Finally, in Sec. V the main conclusions are summarized.

II. THERMODYNAMICS

Let a generic thermodynamic closed system be described by temperature, T, and generalized forces, $\{\mathbf{y}_i\}_{i=1..n}$, as independent variables. Differential changes of these variables lead to a differential change of entropy that can be written as

$$dS(T,\{\mathbf{y}_i\}) = \frac{C}{T}dT + \sum_{i=1}^{n}\left(\frac{\partial S}{\partial \mathbf{y}_i}\right)_{T,\{\mathbf{y}_{j\neq i}\}} d\mathbf{y}_i, \qquad (1)$$

where we have taken into account the definition of the heat capacity $C = T(\partial S/\partial T)_{\{\mathbf{y}_i\}}$. On the other hand, from Maxwell's equations we know that

$$\left(\frac{\partial S}{\partial \mathbf{y}_i}\right)_{T,\{\mathbf{y}_{j\neq i}\}} = \left(\frac{\partial \mathbf{X}_i}{\partial T}\right)_{\{\mathbf{y}_i\}}, \qquad (2)$$

where $\{\mathbf{X}_i\}$ are the generalized displacements thermodynamically conjugated of the forces $\{\mathbf{y}_i\}$. The caloric effect associated with the property $\mathbf{X}_i$ can be quantified as the isothermal entropy change and the adiabatic temperature change associated with a variation of the conjugated field $\mathbf{y}_i$ (for instance, from 0 to a given finite value). These changes can be written as

$$\begin{aligned}\Delta S(0\rightarrow \mathbf{y}_i) &= S(T,\mathbf{y}_i,\{\mathbf{y}_{j\neq i}\}) - S(T,0,\{\mathbf{y}_{j\neq i}\}) \\ &= \int_0^{\mathbf{y}_i}\left(\frac{\partial \mathbf{X}_i}{\partial T}\right)_{\{\mathbf{y}_i\}} d\mathbf{y}_i, \end{aligned} \qquad (3)$$

and

$$\begin{aligned}\Delta T(0\rightarrow \mathbf{y}_i) &= T(T_{\text{in}},\mathbf{y}_i,\{\mathbf{y}_{j\neq i}\}) - T(\mathbf{y}_i=0,\{\mathbf{y}_{j\neq i}\}) \\ &= -\int_0^{\mathbf{y}_i}\frac{T}{C}\left(\frac{\partial \mathbf{X}_i}{\partial T}\right)_{\{\mathbf{y}_i\}} d\mathbf{y}_i, \end{aligned} \qquad (4)$$

where T_{in} is the initial temperature of the adiabatic process.

In the present paper, the generalized forces of interest are the magnetic field $\mu_0 H$ (where μ_0 is the magnetic permeability of free space) and the uniaxial stress σ and thus, the corresponding thermodynamically conjugated displacements are the magnetization M and the strain ε.[23] In this case, let $\delta S(\sigma,H)$ be the difference between the stress-induced entropy change at a constant applied field H and the corresponding change at zero applied magnetic field,

$$\begin{aligned}\delta S(\sigma,H) = &[S(T,\sigma,H) - S(T,0,H)] \\ &- [S(T,\sigma,0) - S(T,0,0)]. \end{aligned} \qquad (5)$$

This equation indicates that the magnetic field-induced entropy change at a given constant applied stress is given by

$$\begin{aligned}S(T,\sigma,H) - S(T,\sigma,0) = &\,\delta S(\sigma,H) \\ &+ [S(T,0,H) - S(T,0,0)], \end{aligned} \qquad (6)$$

where the last term in the above equation is the magnetic field-induced entropy change in the absence of applied stress. Therefore, we obtain that the effect of the magnetostructural coupling is accounted for by $\delta S(\sigma,H)$.

III. EXPERIMENTAL DETAILS

A polycrystalline $Ni_{50.5}Mn_{21.7}Ga_{24.7}Co_{3.1}$ (with an electron to atom ratio $e/a = 7.589$) ingot was obtained by arc melting pure metals under an argon atmosphere. Slices cut from the ingot were encapsulated under vacuum in quartz glass, they were annealed at 1073 K for 72 h, and they were subsequently quenched in iced water. From the annealed slices, specimens were spark machined for length change and calorimetric measurements. The sample for length change measurements was a parallelepiped with length $L_0 = 4.39$ mm and cross section $\phi = 4.05$ mm^2 ($m \sim 0.14$ g). A small sample of mass 88.6 mg was used for calorimetric measurements.

The studied alloy undergoes a martensitic transition on cooling starting at $M_s = (272 \pm 1)$ K (in the absence of applied mechanical and magnetic fields).

In Fig. 1 we show ac-magnetic susceptibility and calorimetric (inset) data recorded during heating and cooling runs. On cooling, a sharp decrease of susceptibility is observed at the martensitic transition which reflects the increase of

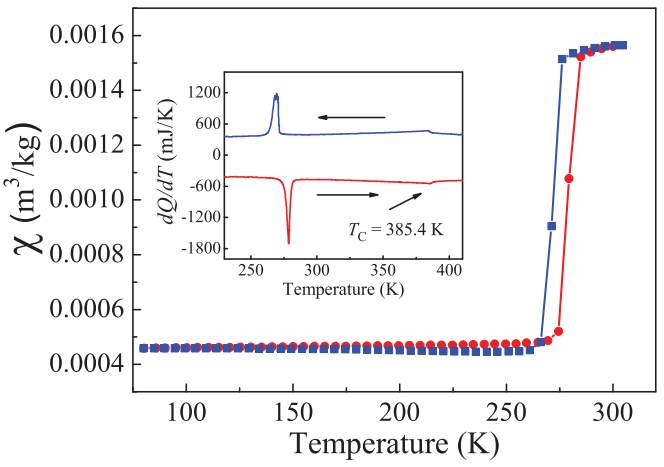

FIG. 1. (Color online) Ac-magnetic susceptibility versus temperature recorded during cooling (solid squares) and heating (solid circles) runs. The inset shows calorimetric curves during cooling and heating.

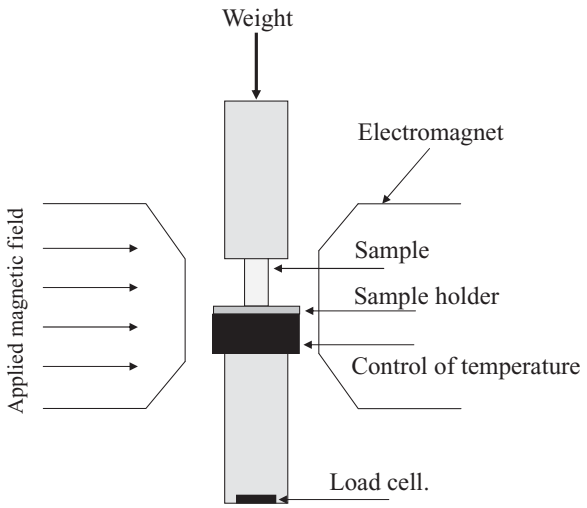

FIG. 2. Schematic representation of the experimental setup, consisting of an electromagnet and temperature-controlled sample holder. The compression stress is applied by means of a weight put on top of the upper rod.

magnetocrystalline anisotropy of the low temperature phase. The transition occurs with a relatively low hysteresis of about 10 K. From the calorimetric data we have computed an entropy change at the martensitic transition (in the absence of externally applied fields) of $\Delta S = (15.8 \pm 0.3)$ J/kg K. The small peak observed on the calorimetric curves at high temperature corresponds to the paramagnetic-ferromagnetic transition at the Curie point, $T_C = 385.4 \pm 0.2$ K.

The experimental setup used to measure length change versus temperature under applied compression stress and magnetic field is schematically shown in Fig. 2. A temperature-controlled sample holder is placed between two cylindrical rods made of a high strength polyamide nylon (nylamid 6/6). The upper rod is in direct contact with the upper surface of the sample. The sample is located between the poles of an electromagnet with a gap of 55 mm that enables the application of magnetic fields up to 1 T. The whole assembly is conveniently kept aligned and uniaxial compressive forces are applied (perpendicular to the magnetic field) by placing weights of controlled mass on the top end of the upper rod. The load was measured by a load cell at the bottom end of the lower rod, which lies on the surface of the bench. A capacitive strain gauge is attached to the upper (mobile) rod to measure length changes. The weight of the rods, sample, and sample holder was taken into account by proper calibration. The transition is thermally induced at given values of the applied magnetic field H and compression force F, which are kept constant during the run.

Stress-induced entropy changes have been computed by taking into account Eq. (3) and for each applied magnetic field, an isothermal stress-induced entropy change has been obtained as

$$\Delta S(T,\sigma,H) = \frac{1}{\rho}\int_0^{\sigma}\left(\frac{\partial\varepsilon}{\partial T}\right)_{\sigma} d\sigma = \frac{1}{m_0}\int_0^{F}\left(\frac{\partial L}{\partial T}\right)_{F} dF, \qquad (7)$$

where $m_0 = \rho\Omega_0$ is the mass of the gauge portion of the sample and $\Omega_0 = \phi L_0$, the corresponding volume. The cross section ϕ is assumed constant. $F = \phi\sigma$ is the applied force and σ the applied stress. The strain is given by $\varepsilon = \Delta L/L_0$, with $\Delta L = L - L_0$, where L is the actual gauge length and L_0 the corresponding length in the absence of applied fields. It is worth noting that the polycrystalline nature of the studied sample and the anisotropic deformation of the martensitic variants lead to an inhomogeneous stress distribution inside the sample. For that reason, the suitable thermodynamic variables to evaluate elastocaloric properties are the macroscopic length change and the applied force which conveniently describe any thermodynamic system subjected to a uniaxial force regardless of the microscopic mechanism responsible for the change in length.

Length change measurements were complemented with calorimetric measurements under an applied magnetic field that enables estimation of magnetic field-induced isothermal changes of entropy. To this end, we have used a specially designed differential scanning calorimeter that enables application of magnetic fields up to 1 T, while temperature is swept at rates of ~0.5 K/min.[24] From the calorimetric curves the variation of entropy along the transition referred to the entropy of the low-temperature phase is obtained as $S(T,H) = \int_{T_i}^{T} \frac{1}{T}\frac{dq}{dT} dT$, where dq/dT is the heat released (or absorbed) per unit temperature and T is a temperature in the range over which the transition extends. T_i is either the starting transition temperature on heating or the finishing transition temperature on cooling.

IV. RESULTS AND DISCUSSION

Figure 3 illustrates a typical example of a measured length as a function of temperature for a magnetic field of 0.36 T, and selected applied stresses up to ~10 MPa.[25] For temperatures above and below the transition region, the length linearly increases with temperature. The shrinkage associated with

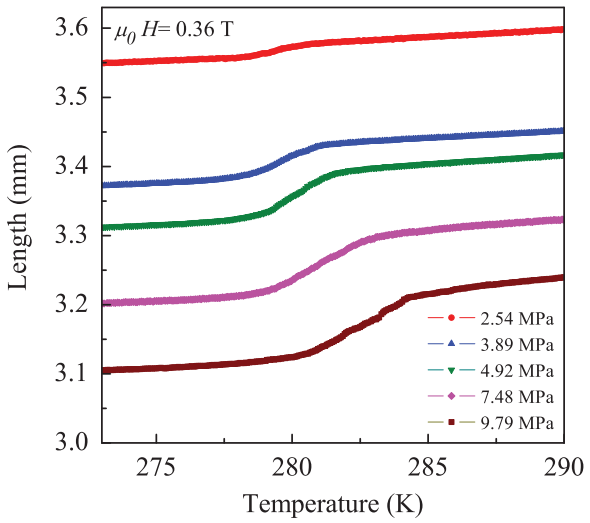

FIG. 3. (Color online) Example of curves giving the measured length vs temperature obtained during heating runs at the indicated values of the applied compression stress and for an applied magnetic field of 0.36 T. See Ref. 25.

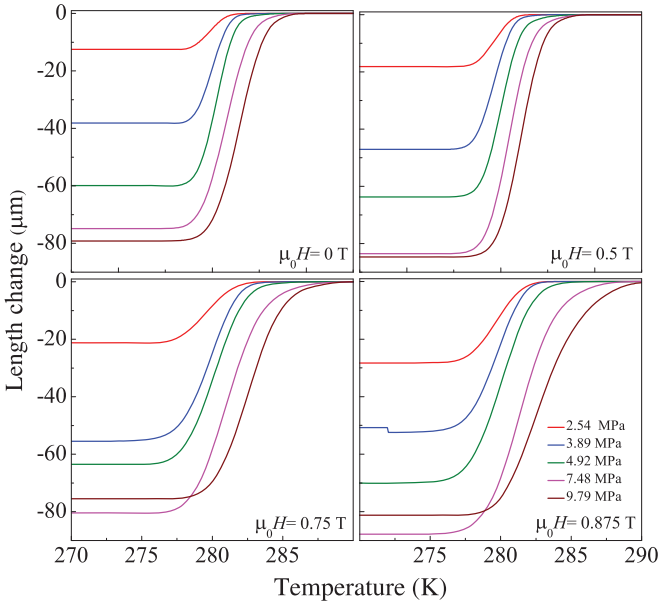

FIG. 4. (Color online) Length change vs temperature curves after correction from the temperature dependence away from the transition region. For convenience, the origin has been taken in the high-temperature parent phase.

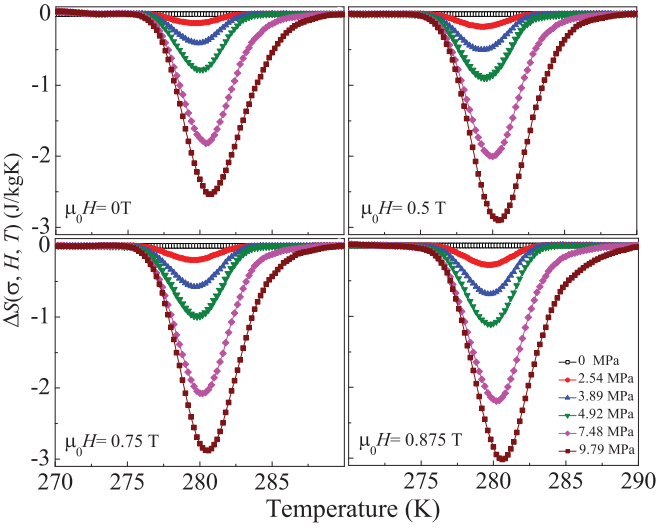

FIG. 5. (Color online) Stress-induced entropy changes at different values of the stress and selected values of the applied magnetic field. Data correspond to heating runs.

the martensitic transition can be obtained by suppression of the temperature change outside the transition region. Results at different magnetic fields and selected applied stresses are shown in Fig. 4. A first evident effect of increasing the compression stress is to increase the stability of the martensitic phase thereby shifting the transition to higher temperatures. On the other hand, the total shrinkage associated with the transition also increases with increasing applied stress. This result reflects the tendency of the stress to break the degeneracy associated with the symmetry-allowed martensitic variants which are equivalent in the absence of applied external magnetic and mechanical fields. Hence, within each grain, the increase of applied stress gives rise to a gradual increase in the fraction of martensitic variants which are crystallographically oriented in a direction energetically favorable to the direction of the applied uniaxial stress.

From the data shown in Fig. 4 we computed the isothermal stress-induced entropy changes as a function of temperature and stress using Eq. (7). Results are shown in Fig. 5 for the selected applied fields. There is a decrease in entropy (negative values for the stress-induced entropy changes) under the application of compressive stress. Such an entropy decrease would result in a temperature increase of the sample [see Eqs. (3) and (4)] for an adiabatically applied stress. This is the most commonly found situation for the several caloric effects for which cooling is achieved upon removing the external field. In this sense the elastocaloric effect found here is conventional. It is worth noting that conventional caloric effects will be found in the cases when the transition temperature increases with external field. Conversely, a decrease in the transition temperature with external field yields to the so-called inverse caloric effect for which the sample cools down under adiabatically applying an external field.

The effect of magnetic field on the elastocaloric effect is illustrated in Fig. 5. The magnetic field enhances the elastocaloric effect: The absolute value of the entropy change for a given stress increases with increasing magnetic field. For the ranges of stresses and magnetic fields investigated, the entropy changes associated with the elastocaloric effect are significantly lower than the whole available entropy content (the transition entropy change) of about 15 J/kg K. Such a low value is a consequence of the fact that the transition is spread over a relatively broad range of temperatures (see Fig. 4) and therefore relatively large fields (stress and magnetic) are required to induce the whole transition. These kinds of large stresses cannot by applied to magnetic Heusler shape memory alloys owing to their brittleness. In contrast, for nonmagnetic ductile shape memory alloys it has been shown that larger stresses induce the transformation of the whole sample and the entropy change associated with the elastocaloric effect coincides with the transition entropy change.[13]

A meaningful parameter for practical applications of caloric effects is the relative cooling power (RCP).[3] For the elastocaloric effect it can be estimated as

$$RCP = \int_{\Delta T} \Delta S(\sigma, H, T) dT, \tag{8}$$

where the range over which the integral is performed, ΔT, corresponds to the extension of the peaks giving the stress-induced entropy changes shown in Fig. 5. In Fig. 6 we plot the obtained RCP as a function of the applied stress for selected values of the applied magnetic fields. Again, the effect of magnetic field is to enhance the elastocaloric effect by increasing the RCP. It is remarkable that after a moderate increase at very low stresses, the RCP increases very steeply with applied stress. Such an increase is due to two contributions. On the one hand, by increasing stress a larger amount of the sample transforms isothermally to martensite thus giving rise to larger stress-induced entropy changes. For large enough stresses this contribution is expected to saturate when the whole sample transforms to martensite. On the other

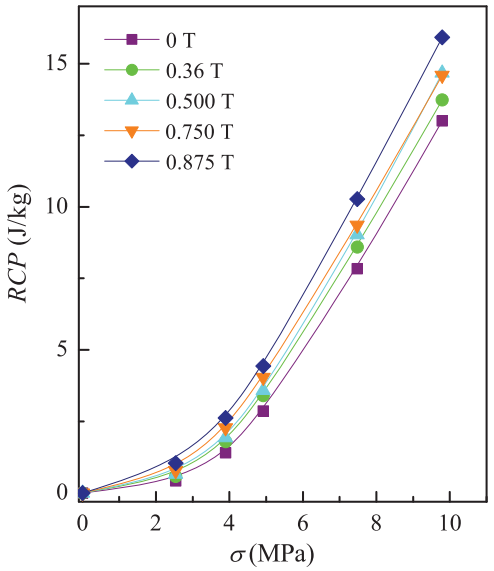

FIG. 6. (Color online) Relative cooling power as a function of the applied compression stress for selected values of the applied magnetic field. Continuous lines are a guide to the eye.

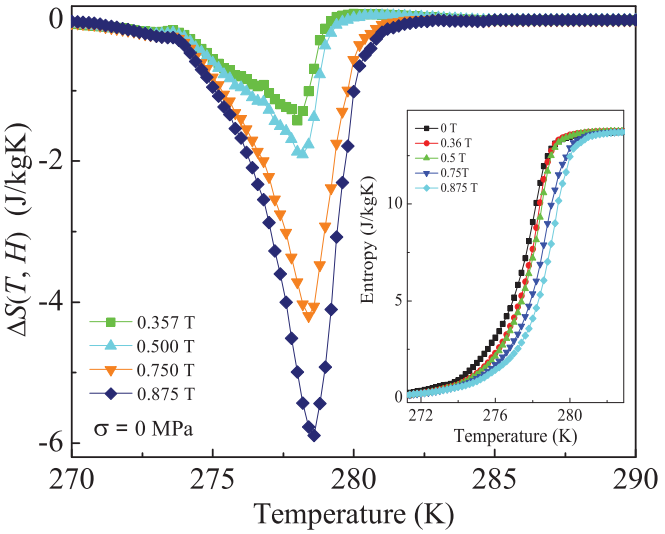

FIG. 7. (Color online) Magnetic field-induced isothermal entropy change as a function of temperature for selected applied magnetic fields and zero compression stress. The inset shows the entropy curves obtained from the calorimetric measurements during heating at the corresponding applied magnetic fields.

hand, the integration range ΔT in Eq. (8) also increases with stress mainly due to the shift in the transition temperature with stress.

At this stage it is interesting to compare the obtained results for the elastocaloric properties of the studied Ni-Mn-Ga-Co system with its magnetocaloric properties. For such a purpose, we estimated magnetic field-induced isothermal changes of entropy at zero-applied stress from differential temperature-scanning calorimetric measurements performed at applied selected magnetic fields up to 1 T. It is worth noticing that DSC calorimetry under a magnetic field has been successfully used to determine entropy changes associated with first-order magnetostructural phase transitions.[24,26–28] Figure 7 shows the obtained magnetic field-induced entropy changes (magnetocaloric effect) as a function of temperature, for selected values of the magnetic field. These data are obtained by subtraction of the transition entropy vs temperature curves at constant field, shown on the inset. The magnetocaloric effect for Ni-Mn-Ga-Co samples with composition close to the one studied here have been reported from magnetization data in Ref. 29. At low fields a small positive entropy change of about 1.2 J/kg K for 1 T was reported. This value decreased for larger magnetic fields and was attributed to be due to the larger magnetocrystalline anisotropy of the martensite. The magnetocaloric effect for the investigated sample is significantly larger ($\sim$ 6 J/kg K for about 1 T) and conventional: negative entropy values over all range of studied magnetic fields. This is consistent with the increase in transition temperature with magnetic field (see inset of Fig. 7). It is worth noticing that the situation is similar to that found for the elastocaloric effect: the range of studied magnetic fields is not large enough to fully induce the transformation of the whole sample and consequently the values found for the magnetic field-induced entropy change are lower than the transition entropy change. The magnetocaloric effect for the largest available magnetic field ($\sim$1 T) is larger than the elastocaloric at $\sim$10 MPa, but is still only a fraction of the overall entropy change. The larger value of the magnetocaloric effect is simply a consequence of the fact that the transition occurs in a narrower range of temperatures in the sample used for calorimetric measurements (the range is approximately half of the range obtained in length change measurements). Therefore, the estimated RCP is rather comparable in both cases. Actually, the same RCP is obtained at $\sigma = 10$ MPa and $H = 0$, and for an applied field of 0.8 T and zero stress.

V. SUMMARY AND CONCLUSIONS

We have reported on the elastocaloric effect in magnetic shape memory alloys. We have also investigated the influence of applied magnetic fields on this effect, and a comparative study with the magnetocaloric effect exhibited by the alloy was performed. Both the elastocaloric and magnetocaloric effects are a consequence of the martensitic transition undergone by the alloy. The effect of a compressive stress and of a magnetic field is to increase the stability of the martensitic phase, thereby leading to an increase of the transition temperature with stress and magnetic field. Consistent with this finding, both elastocaloric and magnetocaloric effects are conventional (i.e., isothermal application of an external field causes a reduction in the entropy of the sample).

The entropy values associated with the elastocaloric effect for relatively low applied stresses (about 10 MPa) are only a fraction of the whole available entropy content owing to the fact that the investigated range of stresses is not large enough to induce the transformation of the whole sample. Actually the brittleness of magnetic shape memory alloys is one of the major drawbacks for the practical application of the magnetic shape memory effect, and efforts are devoted to finding materials with improved mechanical performances. An increase in the

range of applied stresses will result in an enhancement of the elastocaloric effect in magnetic shape memory materials.

The effect of magnetic field is to enhance the elastocaloric effect, particularly for the cooling capacity associated with this effect. It has been found that the cooling capacity increases steeply with applied stress, and therefore this quantity is expected to be significantly increased in the event of finding magnetic shape memory materials with improved mechanical properties.

ACKNOWLEDGMENTS

This work was supported by CICyT (Spain) under Project No. MAT2010-15114.

[1] J. F. Nye, *Physical Properties of Crystals* (Oxford University Press, New York, 1957).
[2] A. M. Tishin and Y. I. Spichkin, *The Magnetocaloric Effect and Its Applications* (Institute of Physics, Bristol and Philadelphia, 2003).
[3] K. A. Gschneidner, V. K. Pecharsky, and A. O. Tsokol, Rep. Prog. Phys. **68**, 1479 (2005).
[4] E. Brück, in *Handbook of Magnetic Materials*, Vol. 17, edited by K. H. J. Buschow (Elsevier, Amsterdam, 2007), p. 235.
[5] S. G. Lu and Q. M. Zhang, Adv. Mater. **21**, 1983 (2009).
[6] N. A. de Oliveira and P. J. von Ranke, Phys. Rep. **489**, 89 (2010).
[7] V. K. Pecharsky and K. A. Gschneidner, Phys. Rev. Lett. **78**, 4494 (1997).
[8] O. Tegus, E. Brück, K. H. J. Buschow, and F. R. de Boer, Nature (London) **415**, 150 (2002).
[9] V. Provenzano, A. J. Shapiro, and R. D. Schull, Nature (London) **429**, 853 (2004).
[10] T. Krenke, E. Duman, M. Acet, E. F. Wassermann, X. Moya, L. Mañosa, and A. Planes, Nature Mater. **4**, 450 (2005).
[11] S. B. Shen, J. R. Sun, F. X. Hu, H. W. Zhang, and Z. H. Chen, Adv. Mater. **21**, 4545 (2009).
[12] A. S. Mischenko, Q. Zhang, J. F. Scott, R. W. Whatermore, and N. D. Mathur, Science **311**, 1270 (2006).
[13] E. Bonnot, R. Romero, L. Mañosa, E. Vives, and A. Planes, Phys. Rev. Lett. **100**, 125901 (2008).
[14] D. E. Soto-Parra, E. Vives, D. González-Alonso, L. Mañosa, A. Planes, R. Romero, J. A. Matutes-Aquino, R. A. Ochoa-Gamboa, and H. Flores-Zúñiga, Appl. Phys. Lett. **96**, 071912 (2010).
[15] L. Mañosa, D. González-Alonso, A. Planes, E. Bonnot, M. Barrio, J.-L. Tamarit, S. Aksoy, and M. Acet, Nature Mater. **9**, 478 (2010).
[16] A. Planes, L. Mañosa, and M. Acet, J. Phys. Condens. Matter **21**, 233201 (2009).
[17] K. Ullakko, J. K. Huang, C. Kantner, R. C. O'Handley, and V. V. Kokorin, Appl. Phys. Lett. **69**, 1966 (1996).
[18] A. Sozinov, A. A. Likhacher, N. Lanska, and K. Ullakko, Appl. Phys. Lett. **80**, 1746 (2002).
[19] R. Kainuma, Y. Imano, W. Ito, Y. Sutou, H. Morito, S. Okamoto, S. Kitakami, O. Oikawa, A. Fujita, T. Kanomata, and K. Ishida, Nature (Lodnon) **439**, 957 (2006).
[20] T. Krenke, E. Duman, M. Acet, E. F. Wassermann, X. Moya, L. Mañosa, A. Planes, E. Suard, and B. Ouladdiaff, Phys. Rev. B **75**, 104414 (2007).
[21] J. Marcos, L. Mañosa, A. Planes, F. Casanova, X. Batlle, and A. Labarta, Phys. Rev. B **68**, 094401 (2003).
[22] D. E. Soto-Parra, X. Moya, L. Mañosa, H. Flores-Zuñiga, F. Alvarado Hernández, R. A. Ochoa-Gamboa, J. A. Matutes-Aquino, and D. Ríos-Jara, Philos. Mag. **90**, 2771 (2010).
[23] Notice that H and σ should have vectorial and tensorial (rank 2) character, respectively. However, we will assume them as scalars and thus the generalized displacements M and ε will be the components corresponding to these fields.
[24] The calorimeter used in the present study is a simplified version, adequate for near-room-temperature measurements, of the calorimeter described in J. Marcos, F. Casanova, X. Batlle, A. Labarta, A. Planes, and L. Mañosa, Rev. Sci. Instrum. **74**, 4768 (2003).
[25] Since the length is obtained from the displacement of the upper rod, it is measured with respect to an arbitrary origin. Its variation with temperature takes into account the length change of the specimen due to the transition.
[26] T. Plackowski, Y. Wang, and A. Junod, Rev. Sci. Instrum. **73**, 2755 (2002).
[27] S. Jeppesen, S. Linderoth, N. Pryds, L. Theil Kuhn, and J. Buch Jensen, Rev. Sci. Instrum. **79**, 083901 (2008).
[28] V. Basso, C. Sasso, and M. Küpferling, Rev. Sci. Instrum. **81**, 113904 (2010).
[29] A. M. Gomes, M. Khan, S. Stadler, N. Ali, I. Dubenko, A. Y. Takeuchi, and A. P. Guimarães, J. Appl. Phys. **99**, 08Q106 (2006).